October 17, 2010

Infrared Excess Emission of OB stars in Cyg OB2 Association

Mark Ma[1], Dae-Sik Moon[1]

ABSTRACT

Fitting of OB stars in Cyg OB2

Subject headings: O type Stars, B type Stars, Excess Emission

1. Introduction

2. Data

A total of 79 stars were studied. 58 of the stars are spectral type B stars, and the remaining 21 stars are spectral type O stars. The position, spectral type and extinction information of these stars were taken from previous works on the Cyg OB2 association by Kiminki et al (2006) and Negueruela et al (2008). The positions of these stars relative to the center of Cyg OB2 association is shown by Fig. 2.

The flux of J, H and Ks bands of the stars were retrieved by querying the published 2MASS catalogue for sources that lies within 2 arc-seconds of the stars. Each of the stars were found to have exactly one counterpart in the 2MASS point source catalogue. The results of the 2MASS photometry are listed in table 3.

Flux at 3.6um, 4.5um, 5.8um and 8um are gathered using the data from Spitzer Space Telescopes (SST) IRAC instrument. Our source Fits file were downloaded Basic Calibration Data (BCD) from the SST archives. Aperture photometry were performed on each individual BCD fits files in accordance to the steps outlined in the SSTs IRAC Instrument Handbook. The validity of the flux measurement is verified by performing the same flux measurement on sources published in GLIMPSE catalogue and comparing the measured value against the published values in the catalogue. The measured values were found to be within the error of

[1]Department of Astronomy and Astrophysics, University of Toronto, Toronto, ON M5S 3H4, Canada; mark.ma@utoronto.ca, moon@astro.utoronto.ca

the published values and were considered to be accurate. From this we concluded that the flux measurement methods are valid and by extension the measured flux for our Cyg OB2 stars are also reliable.

Flux at 24um are extracted using the MIPS instrument onboard SST. Source fluxes are extracted from Post BCD (PBCD) data using Spitzers APEX software as per MIPS Instrument Handbook instructions. Similar to IRAC data, 24um data verification is done by comparing our performing the flux measurement on sources that have published 24um flux values. We found good agreement in our measured values and the published values, which lead us to conclude that our measurement methods are valid.

12 of the stars are also detected at 9um by Akari, the photometry data for both Spitzer and Akari wavelengths are listed in table 4. (The Akari data are not used in the fittings at this point)

3. Spectral Energy Distribution Fittings

Each star is fitted with simple stellar model. Kurucz models are used for all B type stars and Matins model are used for all O type stars. The expected flux values are computed by convolving the response function of 2MASS, Spitzers IRAC and MIPS instrument with the model. A range of models are assigned to each spectral type based on the estimated temperature and mass of the star. The stars are then fitted with these models using reduced chi squared fit. All stars are allowed a range of discrete extinction values within approx 1 mag Av range of the documented values. The extinction where the best fits occurred is show in the table 4 along with the rest of the fitting parameters. The results of the fit are then used to evaluate the goodness of fit of the stellar flux against models. The stars are sorted into groups depending on the χ^2_R values.

We define group A to be the group containing stars well fitted to the stellar models. Here we define a star with χ^2_R of 2 or less as well fitted to the stellar model. χ^2_R value of 2 was chosen because it is the typical value of a star that has measured flux come to within 2x error of the model predicted values in all wavelengths.

All stars that have failed to make into group A are further fitted twice. The two fittings are independent of each other. One of the fitting has the star fitted with an additional modified blackbody component as a simple approximation to circumstellar dust emissions in addition to the stellar model component.

$$I_d = C \cdot (\frac{2h\nu^2}{c^2})(\frac{1}{exp(\frac{h\nu}{kT}) - 1}) \cdot \nu^{1.5} \quad (1)$$

Where C is a proportionality constant and T is temperature of the modified blackbody in Kelvins.

The other fitting has the star fitted with a power law component approximating stellar wind emission from the star in addition to the stellar model component.

$$I_{sw} = C \cdot \nu^{\gamma} \quad (2)$$

Stars are sorted into further groups depending on the χ^2_R value of the new fittings.

Group B contains stars with good emission fits. These stars has new reduced chi squared value is smaller than 2.

Group C contains stars whose new reduced chi squared value is better than the first time, however the value is still greater than 2.

Group D contains stars with final reduced chi squared value greater than 5. The emissions from this group of stars cannot be accounted for by our modeling.

The SED of each star with fitting are also visually examined to confirm that the fitting is reasonable. Occasionally some stars have reduced chi squared value that is slightly outside of the defined boundary of a certain group, but appears very similar to the group in graphical analysis of the results. These stars are designated borderline cases of that group by the sign (?). The detailed fitting results for each star are listed in table 5.

3.1. Result of O type Stars

Table 1 summarises the SED fitting result of the O type stars with the added dust component.

There are in total 21 O type stars.

Matins stellar models were used to model the stellar flux of the O type stars. In addition, the stars also fitted with a single dust component or a stellar wind component in addition to the stellar model.

We found that O type MSQ stars tends to be well fitted to the stellar model regardless of the presence of 24um detection. O type stars with LC II-IV fitted well after the inclusion

of an excess emission component. O type super giants tends to be unpredictable in which group theyll end up. Each of the stars are discussed in later sections. The fitting result of O type MSQ tends to agree well with that of B type stars without 24um detection in that they are very good fits to the stellar model. This is an indication that flux measurement was consistent and accurate and that the stellar model is also working as expected.

Similar to B type stars, fitting with the stellar wind component did not give better fitting results than dust component and quite often returned worse results.

Group A stars does not show any apparent signs of excess emission. This may be expected with the majority of the MSQ stars, however it is interesting that one early super giant also fitted very well to just the stellar model given that all other super giants we investigated showed some excess emission or at least fitted poorly to the models. Fig **??** shows the SED of the super giant in question, exhibiting a typical SED found in group A stars.

Group B stars shows change after fitting with a dust component model such that the χ^2_R improved to a value less than 2. The typical SED of a group B star usually shows some excess at longer wavelengths, which can be accounted for by a modified blockbody of approx 300K representing emissions from a dust component. The added dust component improved the fit in the wavelength of 3.6um and longer. However in several cases the stars in group B are without 24um detection and therefore without further data at longer wavelength it is difficult to draw conclusion for some of these stars. Fig 4 shows the typical fitting of a group B star.

Group D stars typically fitted extremely poorly to the models. Fig **??** shows the typical emission of a star in group D. The fit is very poor for almost all wavelengths. There is significant excess between 2mass J band to IRAC 8um. The flux at the 24um is significantly less than expected which might be explained by the presence of significant foreground continues emission at the location of this star. Despite all this, a modified blackbody component of around 750k significantly improves the fitting. The fitting at the four IRAC bands are the most improved and results in good fits. The 2Mass and 24um fits continues to be poor. The fitted dust emission contributes up to 17% of the total observed emission at some wavelengths. (Other stars are at 2%)

Table **??** summarises the SED fitting result of the O type stars with the added dust component.

As discussed previously in the dust component fitting for the O type stars, all of the O type MSQ stars fitted well to the Matins stellar model.

The result of free-free component fit showed very little improvement in the goodness of fit with none of the stars being significantly improved by the inclusion of the additional emission component. However it should be noted that all of the O type stars are at least a order of magnitude dimmer than the single BOIa star that showed significant improvement from free-free emission fittings.

Fig **??** shows the typical SED and fitting of a star belonging to group C.

The observed emission at 24um is less than that predicted by the model. The fits at the shorter wavelengths are relatively good, however the added free-free emission component makes very little improvement to the goodness of fit.

More stars falls into group D in the fitting with free-free component compared to the dust component. All the stars that were previously in group D under dust component fitting remained in group D after the free-free component fit. Fig **??** shows the SED and fitting of A15, which was previously shown to fit poorly with the added component.

It is clear that this star fitted very poorly in almost all observed wavelengths, with the worst points of fit occurring at J, H and 24um bands. The added free-free component improved the fit at the short wavelengths but did little to improve the fit at longer wavelengths. This is to be expected as it is clear from the figure that the free-free emission is in the wrong shape to account for the poor fits on at both short and long wavelengths.

3.2. Result of B type stars

Table 2 shows the detailed breakdown of B type star fitting results by group and by luminosity class. as table 2 shows, 15 out of the 16 stars detected at 24um did not fit well with just the stellar model, where as for stars not detected in 24um, 38 out of 42 stars fitted well to the stellar model.

This strongly suggests that the mere detection at 24um of a B type star may indicate some type of emission not accounted for by the model. While not every single star with poor chi squared value automatically implies the presence of excess emission at 24um. Further analysis of the data indicates that contribution by excess emission from a low temperature blackbody source is likely the cause of 44% of the poor fitting results. The details of the analysis will be discussed later in this documentation.

Table 2 also shows that 11 out of the 45 MSQ stars detected in total fitted poorly. A total of 10 MSQ stars were detected at 24um, 9 of these stars fitted poorly, which is consistent with the earlier conclusion that 24um detection leads to poor fits.

33 out of the 35 stars that did not have 24um detection fitted well to just the stellar model. This indicates that the stellar model is valid for B type MSQ stars.

Similarly, stars with luminosity class of II, III and IV fitted poorly for the 2 stars with detection in 24um, and fitted well for the remaining 5 stars. The wellness of fit with the 5 stars without 24um detection again seems to indicate that the model is valid.

Supergiants do not seem to follow the same pattern set by the other stars. None of the stars fitted well with just the stellar model. 3 out of the 6 supergiants fitted well to model and excess emission component. The fit for the remaining 3 super giants remained poor. 4 out of 6 SG stars have detection in 24um, which is the highest detection rate by luminosity class. While all SG stars have fitted poorly to just the stellar model, 24um detection cannot be said to be the cause of the poor fits.

The results seems to indicate that detection of the B type stars of LC II-V at 24um is a strong indication of other emission components affecting the observed flux for MSQ fluxes. Stars with LC between II and IV generally agrees with MSQ stars. However due a very small number of them being detected it is difficult to draw statically meaningful conclusion regarding these stars.

All of the B type supergiants fitted poorly, which would either indicate that SG always have additional emitting components or the Kurucz model is not sufficient to account for the emission of the B type super giant stars.

One frequently occurring feature in the MSQ stars detected in 24um is the presence of very high level of flux at 24um comparable or even higher than those detected at 8um. Kurucz model does not predict an increase in flux at 24um, leading to very poor fitting results. The fluxes are extracted with Spitzer APEX pipeline for MIPS as per instrument handbook instructions, all except one stars have a SNR of at least 10, the extracted flux value should be considered as reliable.

Typical SED fittings for each groups as defined previously are shown below.

Group A stars typically shows the observed fluxes of the star fitting closely to the model predicted value at all wavelengths as shown in fig 3. The majority of the B type MSQ stars without 24um detection fitted well to the stellar model.

Group B stars are stars whose fitting improved after the inclusion of an modified blackbody component accounting for excess emission to a χ^2_R values of 2 or better. Fig **??** shows a typical example of a star in group B.

The typical dust temperature fitted of a MSQ star that fitted well after the dust compo-

nent is around 150-350 Kelvin. Fig **??** shows the high 24um values that seems to be common amongst B type stars with 24um detection.

Amongst the stars in group B, two stars are super giants these stars fitted very well with the added dust component of slight higher temperature at 550K. Fig **??** shows the typical SED of a super giant star that fitted well to the added dust component.

Group C stars included stars that have improved somewhat with the added dust component, but the fit remained poor. Fig. **??** shows the SED of a typical group C star. The star showed improved fitting but dust temperature of 1950k is the ceiling of allowed dust temperature range. From experiences with similar fits in O type stars, such high fitted dust temperature is usually an indication that the fit is invalid.

Group D contains stars that simply did not fit well to the stellar model or any combination of stellar model plus the dust component. Of the 7 stars that did not fit well, 2 are super giants and 2 stars have LC Ve, the remaining 3 stars have low SNR and therefore makes the flux measurement less reliable to other stars. There is not a single typical cause shared amongst the group D stars as the reason of the poor fit.Fig. **??** shows the plot of one of the LC Ve stars.

Table **??** shows a summary of the SED fitting results for B type stars with free-free component added to the stellar model component, there are a total of 19 stars were fitted. Only one of the stars showed enough improvement to be classified as a good fit (Group B) while the remaining stars either improved very little or did not improve at all in goodness of fit. There does not appears to be any relationship in the goodness of fit of the 19 poorly fitted stars and the luminosity class of the stars being fitted. There also do not appear to be any relation in goodness of fit and 24um detection.

Only one star out of 19 fitted well with the added free-free emission component. This star is the brightest star in our entire selection by several orders of magnitude. It may be expected that very bright stars will have certain amount of emissions due to stellar wind. However, even in the best cases the fitting results with stellar wind component is not definitively better than the result obtained with the dust component, so it may be difficult to conclude which component is accountable for the observed excess.

Only one star falls into group B, the SED fitting of the star is shown in fig. **??**.

It is clear by looking at fig **??** (a) that the reason for the poor fit is the observed fluxes deviates significantly from the expected flux in the shorter wavelength bands, particularly the J, H and Ks bands.

The free-free emission component helped to significantly improve the goodness of the fit

from a χ^2_R of 56 from the original fitting to the χ^2_R of 3.6 with free-free emission component. A free-free emission component can make up for much of the differences in flux towards the shorter wavelengths. However, the fit with the free-free component is slightly poor at 5.6um and 8.0um channels due to there being a slightly higher observed flux than the model predicts in those two channels.

The fitted flux component accounts for roughly 10% of the total stellar emission across all of the detected wavelengths.

Fig. **??** shows a typical SED and fits for a star in group C.

As the figure shows, the star fits well to the model in all wavelengths except 24um. The main contributor of the large χ^2_R is the more than expected emission at 24um. Fitting with the free-free component reduces the differences between observed and expected model at 24um, however this is done at the expense of the goodness of fit in other wavelengths. This is mainly due to free-free component decreases with increasing wavelength and therefore is the wrong distribution to properly account for a increase in observed emission at long wavelengths. It should also be noted that the star show in the figure is more than two orders of magnitudes dimmer than the star show in group B.

Group D consists of mainly dim stars in the table with J band dereddened flux of around 1Jy and in particular those with a significant excess at 24um. In addition, all the stars that fitted in group D in the dust component fit remained in group D. Fig **??** shows a typical SED of a star in group D.

The main contributor of the poor fit is at 24um wavelengths. High 24um values similar to this one is also the cause of many B type stars fitting poorly to just the stellar model. From the figure it is clear that the high 24um value cannot be possibly accounted by an added free-free component model because the free-free component contribution decreases as the wavelength increases.

All of the stars in group D are also at least one order of magnitude dimmer than the single star that fitted well to free-free emission in group B. It may be possible that there is a minimum brightness a B type star needs to obtain to have significant excess emissions from free-free emission component.

In comparison, it is clear that the simple dust emission model is much more likely to produce much better fits for the 19 stars that did not fit to just the stellar model. Only the very bright stars in our list shows signs that the free-free emission component produce somewhat comparable fits results as those produced by the dust component.

4. Discussion

5. Conclusion

Based on the fitting results of the 79 stars in total, 30% of the stars showed emission not predicted by the model. This number is quite consistent for both O and B type stars, with 28% of the 21 B type stars fitted poorly and 32% of the 58 B type stars fitted poorly. By process of visual examination it is established that the cause of the poor fit is one or more bands showing more than expected level of flux.

For O type stars the excess emission appeared exclusively in post main sequence stars, whereas in B type stars shown excess emissions in all spectral types. Early type stars appears to be more likely to have excess emission in both spectral types. Super giants stars of both spectral types are very likely to show excess emission, 75% of the 4 O type supergiants showed excess emission, and 100% of the 6 B type supergiants showed excess emission. For other post main sequence stars, O type stars still showed significant tedencies to have excess emission with 66% of 3 stars (sample too small?) showing excess, however the same does not for B type stars of these lumnosity classes with only 28% of 7 stars.

In fitting with the added dust component to the stars that showed excess emission, 42% of the 19 B type stars fitted well and 60% of the 5 O type stars fitted well. In comparision the fitting with the stellar wind component made nearly no improvement in fit to the star that showed excess emission. From the fitting result we can conclude that about half of the star showing excess emission can be accounted for by a simple dust component.

REFERENCES

Douglass, J. W, Young T. T., Hodapp, W. W, Design Review of a Flexure Focus Stage for the Gemini Telescope Near Infrared Imager, 1998, SPIE, 3354, 277

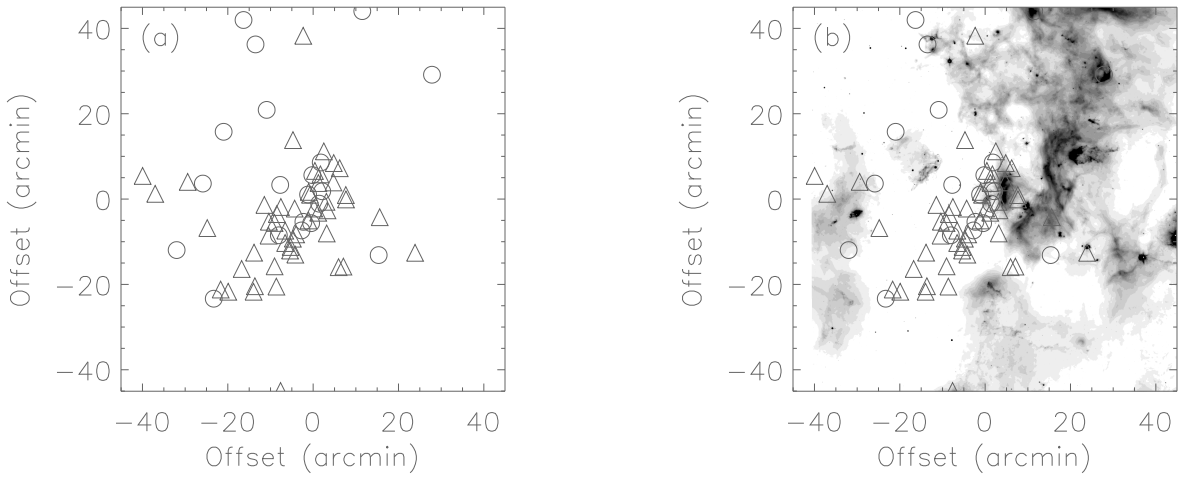

Fig. 1.— Position of the stars studied relative to the center of Cyg OB2 assoication, observed with 2mass at Ks band and Spitzer's MIPS at 24um. B type stars are marked with triangles and O type stars are marked with circles.

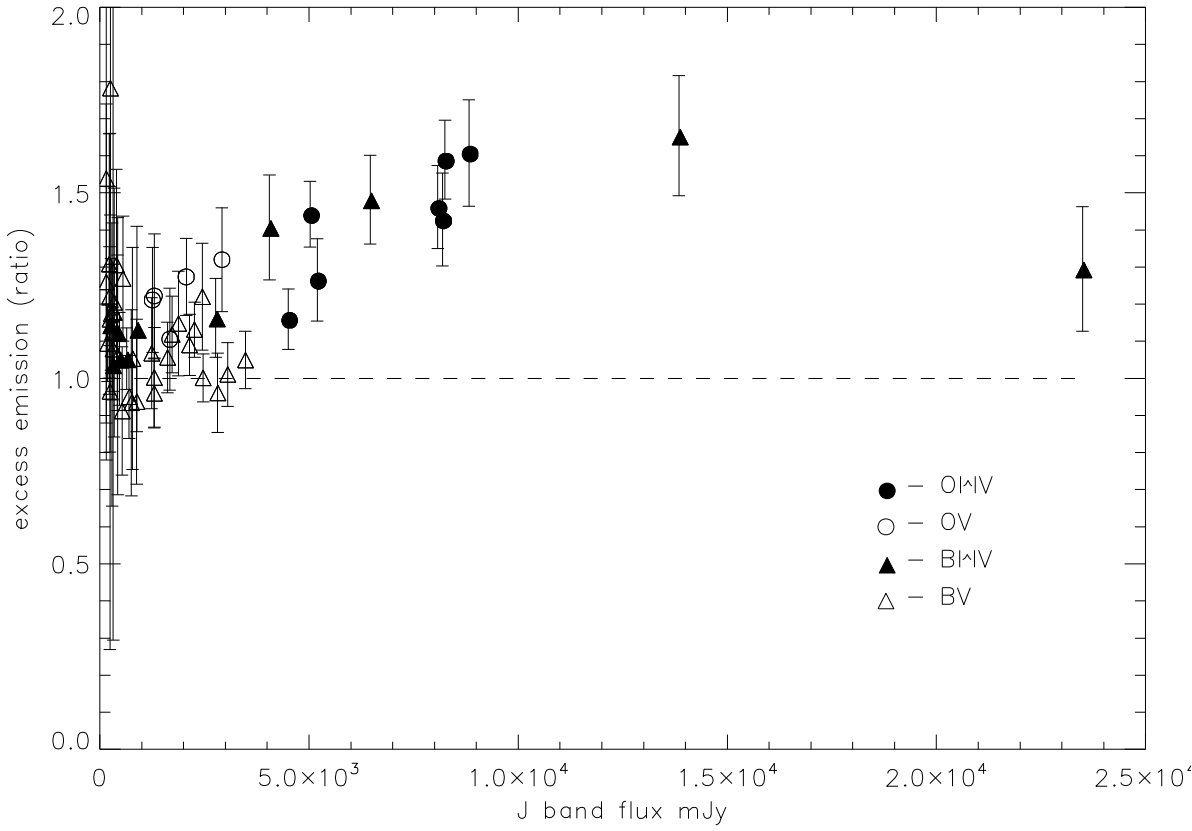
2.0
1.5
1.0
0.5
0.0
excess emission (ratio)
0
5.0×10^3
1.0×10^4
1.5×10^4
2.0×10^4
2.5×10^4
J band flux mJy
– OI^IV
– OV
– BI^IV
– BV

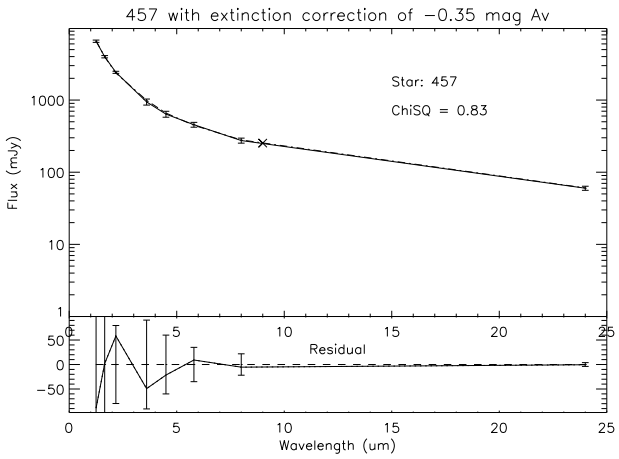

Fig. 3.— Typical SED of Group A star. SED plot of MT457 (O3If) fitted with only a stellar model.

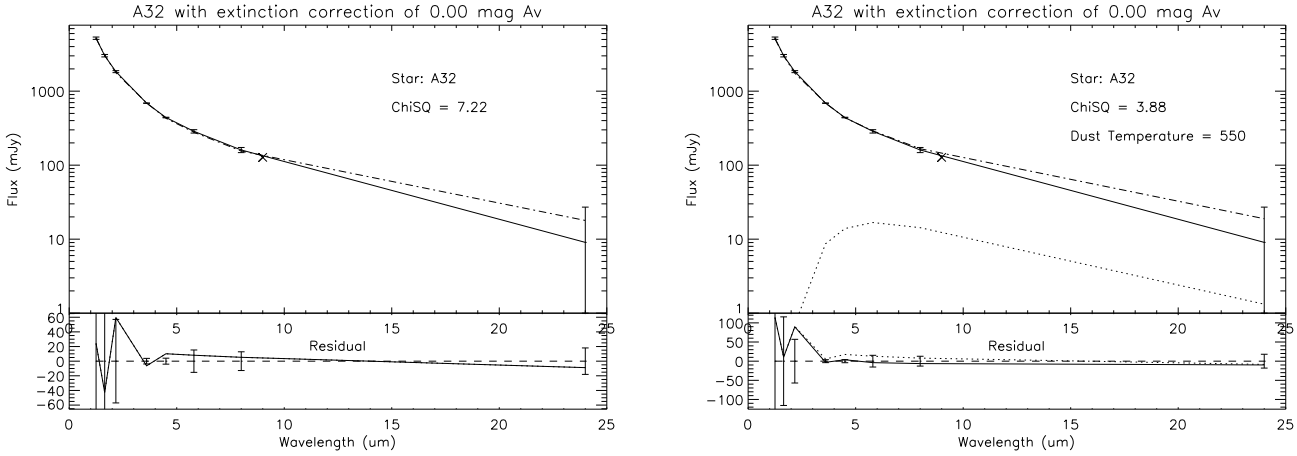

(a) Stellar Model Only

(b) Stellar Model with Dust Component

Fig. 4.— Typical SED of Group B star with dust component. SED plot of A32(O9.5IV), dotted line indicate dust component, dashed line indicate model component.

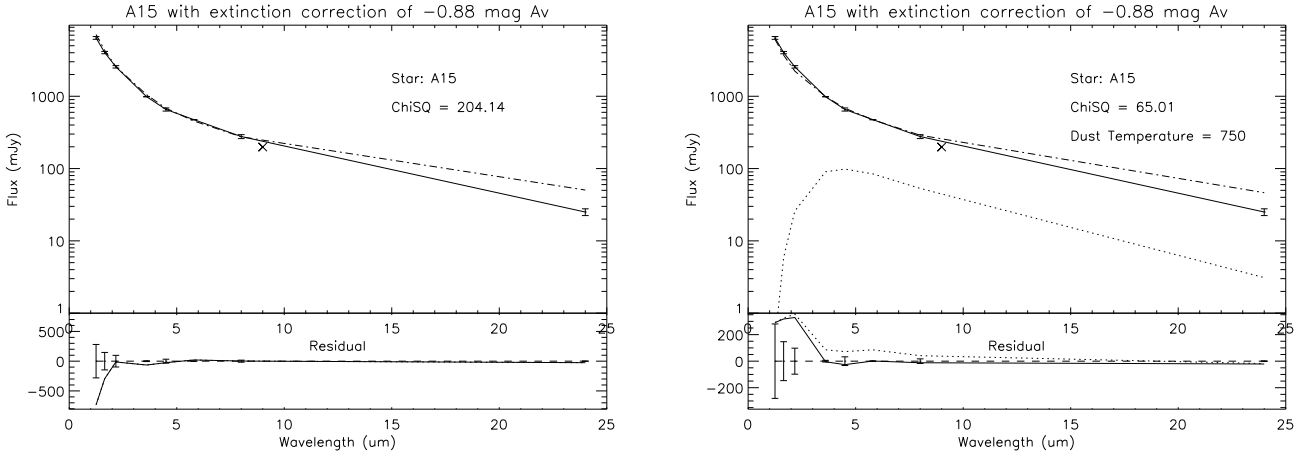

(a) Stellar Model Only

(b) Stellar Model with Dust Component

Fig. 5.— Typical SED of Group D star with dust component. SED plot of A15(O7Ibf), dotted line indicate dust component, dashed line indicate model component.

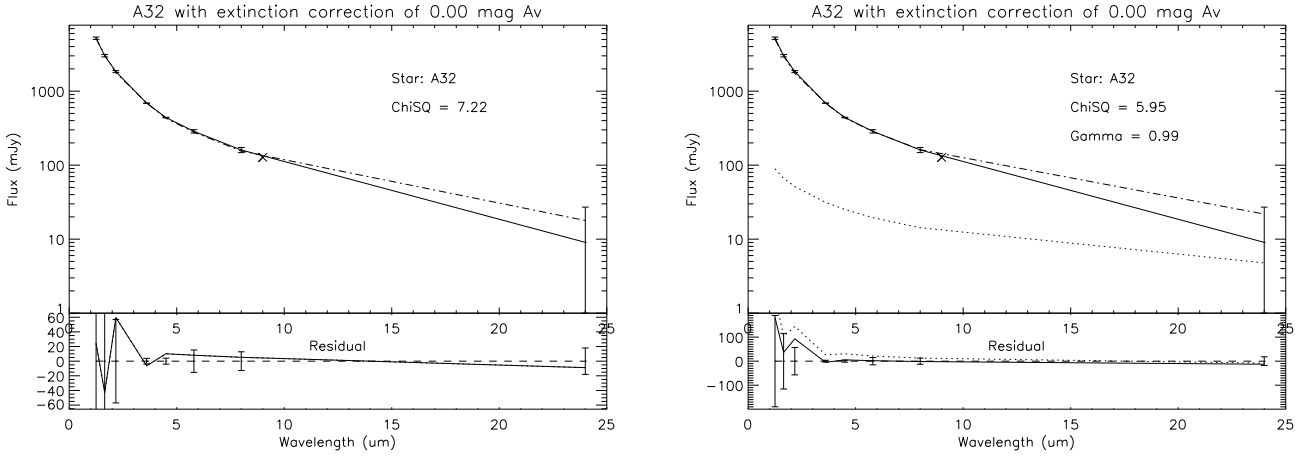

(a) Stellar Model Only

(b) Stellar Model with Free-Free Component

Fig. 6.— Typical SED of Group C star with free free. SED plot of A32(O9.5IV), dotted line indicate dust component, dashed line indicate model component.

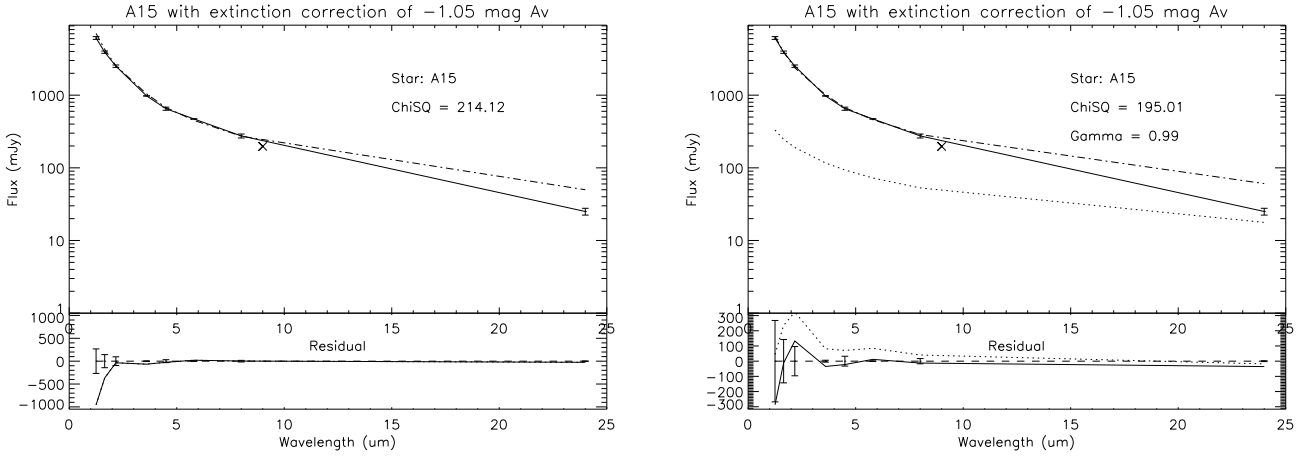

(a) Stellar Model Only

(b) Stellar Model with Free-Free Component

Fig. 7.— Typical SED of Group D star with free free. SED plot of A15(O7Ibf), dotted line indicate dust component, dashed line indicate model component.

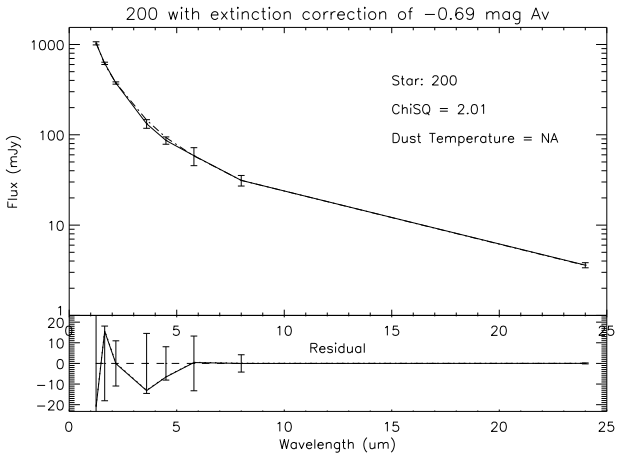

Fig. 8.— Typical SED of Group A star with dust component. SED plot of MT200 (B3V) fitted with only a stellar model.

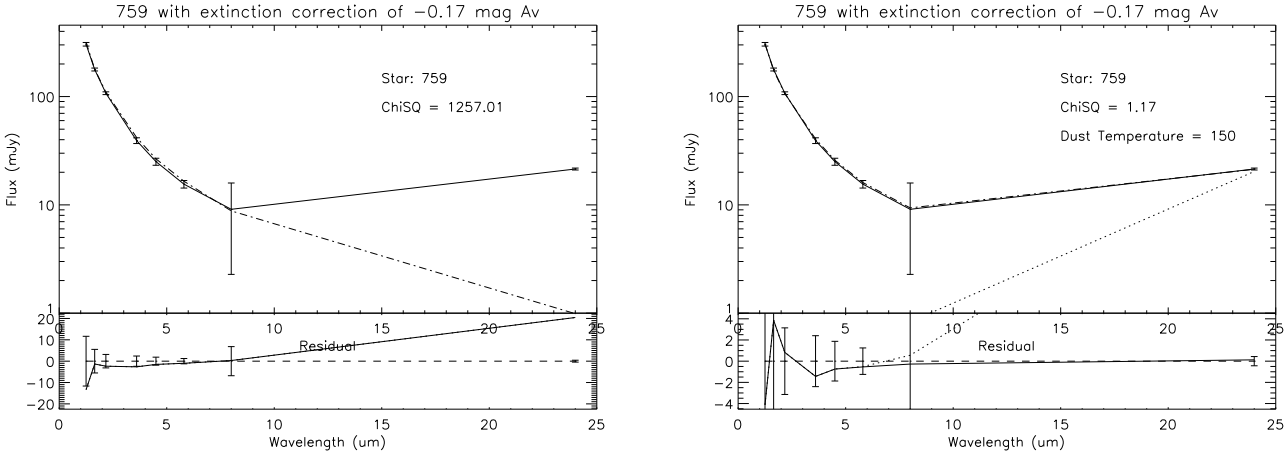

(a) Stellar Model Only

(b) Stellar Model with Dust Component

Fig. 9.— Typical SED of Group B star with dust component. SED plot of MT759 (B1V), dotted line indicate dust component, dashed line indicate model component.

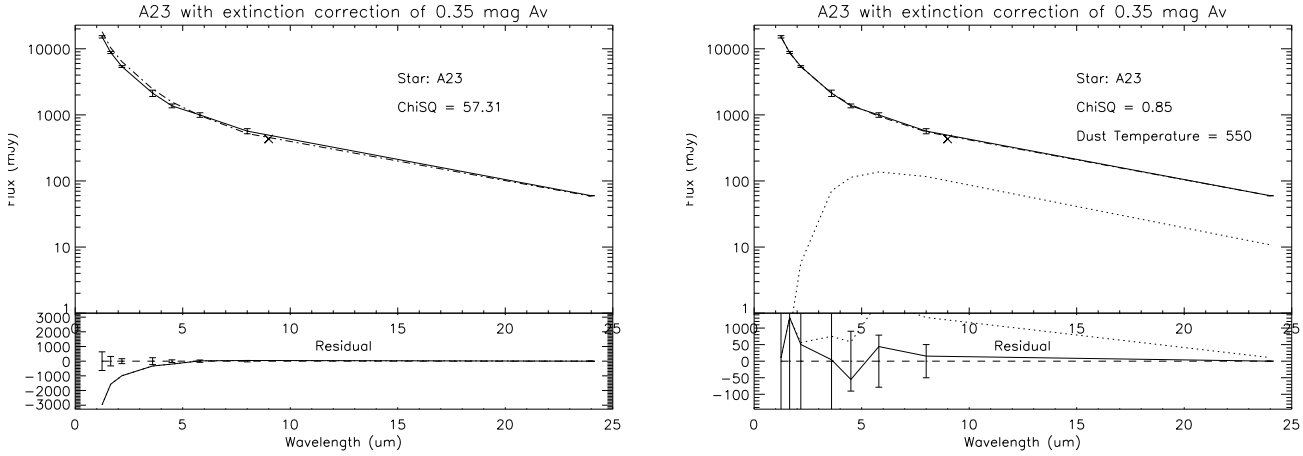

(a) Stellar Model Only

(b) Stellar Model with Dust Component

Fig. 10.— Typical SED of Group B star with dust component. SED plot of A23 (B0.7Ib),dotted line indicate dust component, dashed line indicate model component.

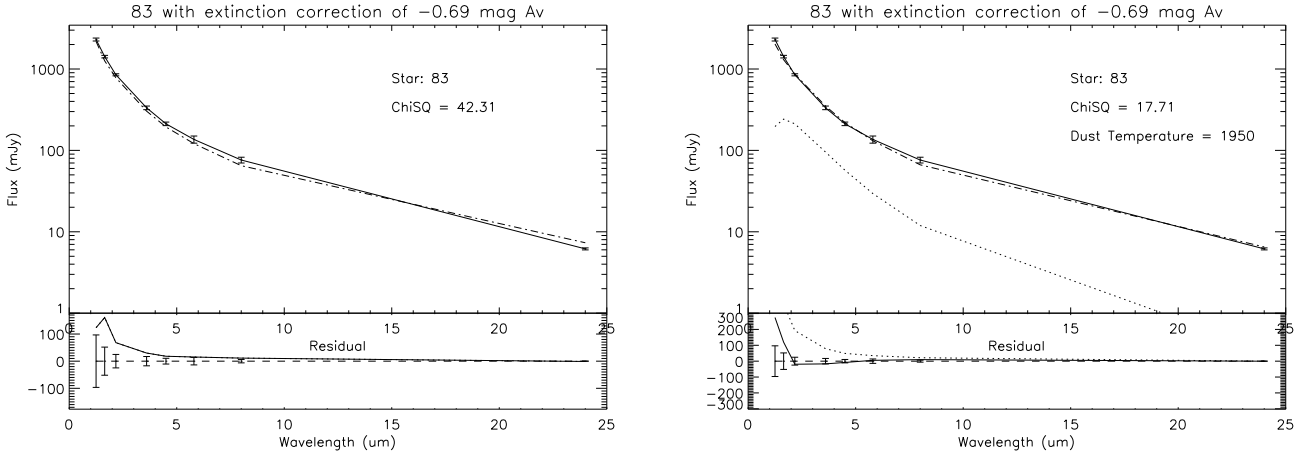

(a) Stellar Model Only

(b) Stellar Model with Dust Component

Fig. 11.— Typical SED of Group C star with dust component. SED plot of MT83 (B1I), dotted line indicate dust component, dashed line indicate model component.

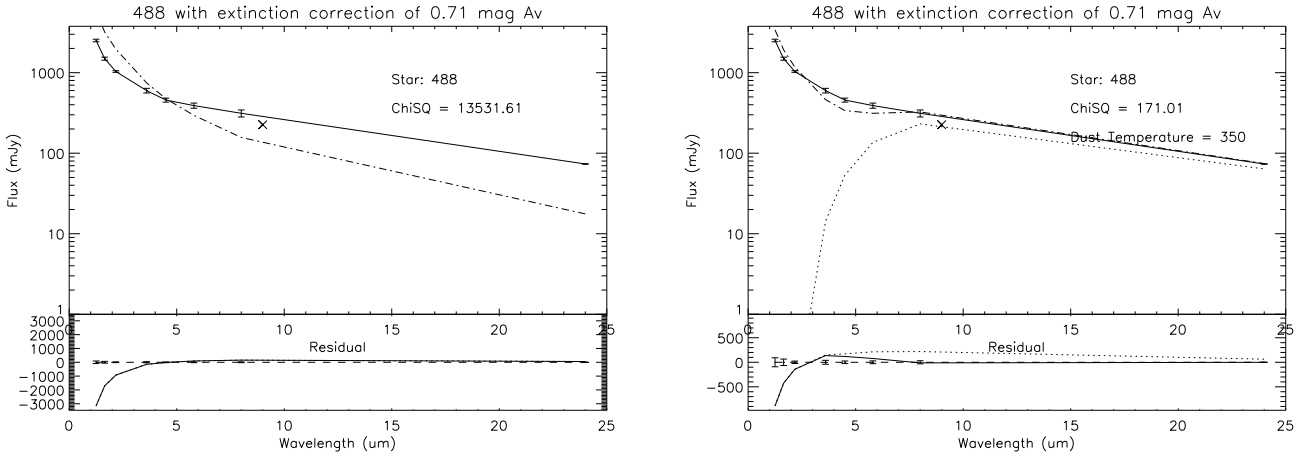

(a) Stellar Model Only

(b) Stellar Model with Dust Component

Fig. 12.— Typical SED of Group B star with dust component. SED plot of MT488 (B1Ve-B3Ve), dotted line indicate dust component, dashed line indicate model component.

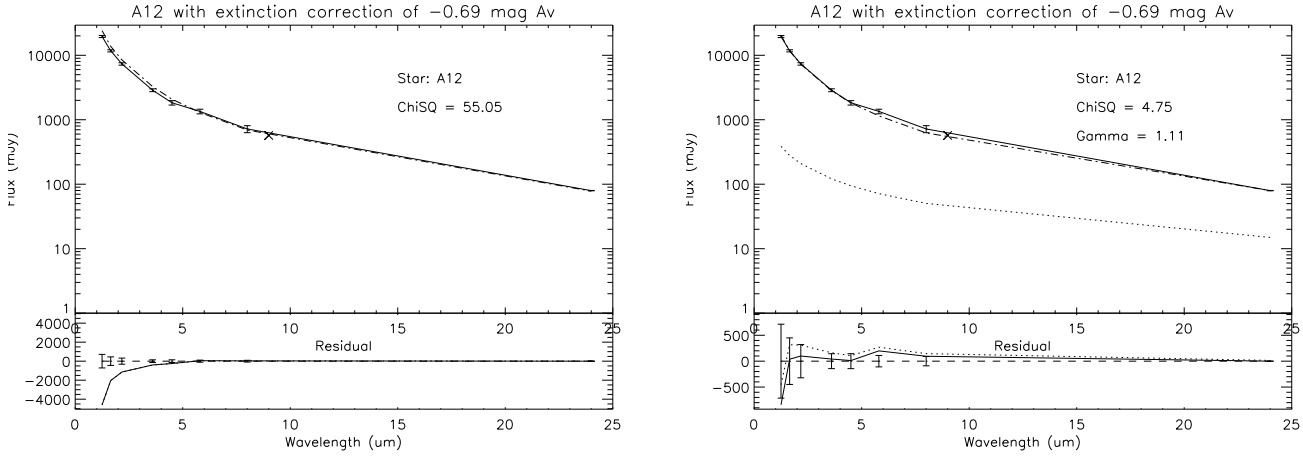

(a) Stellar Model Only

(b) Stellar Model with Free-Free Component

Fig. 13.— Typical SED of Group B star with free free. SED plot of A12 (B0Ia), dotted line indicate free-free component, dashed line indicate model component.

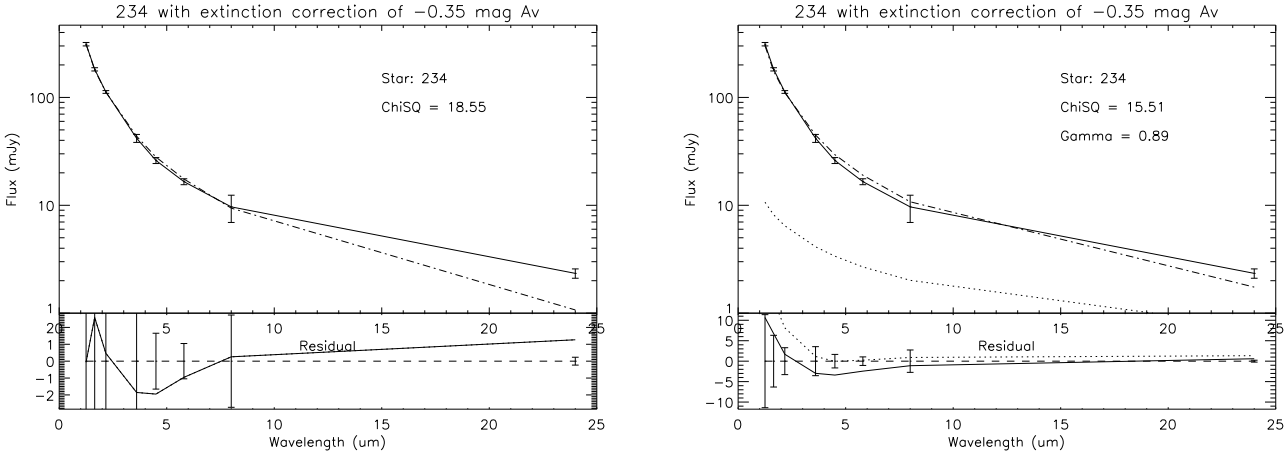

(a) Stellar Model Only

(b) Stellar Model with Free-Free Component

Fig. 14.— Typical SED of Group C star with free free. SED plot of MT234 (B2V), dotted line indicate free-free component, dashed line indicate model component.

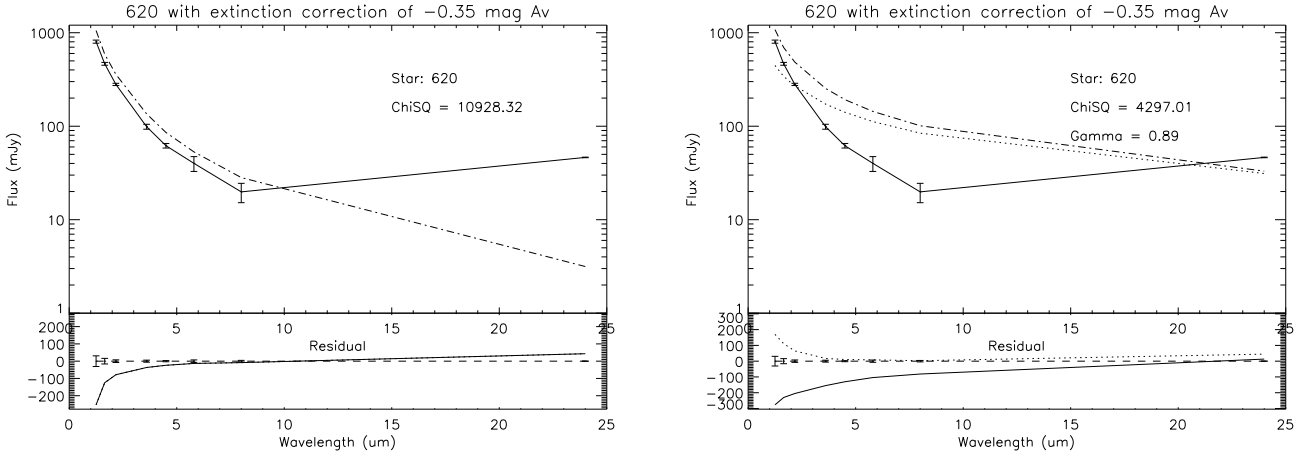

(a) Stellar Model Only

(b) Stellar Model with Free-Free Component

Fig. 15.— Typical SED of Group D star with free free. SED plot of MT620 (B0V), dotted line indicate free-free component, dashed line indicate model component.

Table 1. Summary table for O type stars

Luminosity Class	Group (Dust)				Group (Stellar Wind)				Total
	A	B	C	D	A	B	C	D	
I	1(1)	1(0)	···	2(2)	1(1)	···	···	3(2)	4(3)
II, III, IV	1(0)	2(1)	···	···	1(0)	···	1(1)	1(0)	3(1)
V	14(3)	···	···	···	14(3)	···	···	···	14(3)
Total	16(4)	3(1)	···	2(2)	16(4)	···	1(1)	4(2)	21(7)

Note. — Numbers in parentheses indicate the number of stars detected at 24μm.

Table 2. Summary table for B type stars

Luminosity Class	Group (Dust)				Group (Stellar Wind)				Total
	A	B	C	D	A	B	C	D	
I	···	3(2)	1(0)	2(2)	···	1(1)	3(1)	2(2)	6(4)
II, III, IV	5(0)	1(1)	···	1(1)	5(0)	···	···	2(2)	7(2)
V	34(1)	4(4)	1(1)	6(4)	34(1)	···	1(1)	10(8)	45(10)
Total	39(1)	8(7)	4(2)	7(6)l	39(1)	1(1)	4(2)	14(12)	58(16)

Note. — Numbers in parentheses indicate the number of stars detected at 24μm.

Table 3. Basic Information

Star Index	(R.A.,Dec.)	Spectral Type	Av
MT 5	(20:30:39.90, 41:36:50)	O6V	5.3
MT 20	(20:30:51.10, 41:20:21)	B0V	7.3
MT 21	(20:30:50.80, 41:35:06)	B2II	4.4
MT 42	(20:30:59.40, 41:35:59)	B2V	4.4
MT 83	(20:31:22.00, 41:31:27)	B1I	4.1
MT 97	(20:31:30.50, 41:37:15)	B2V	4.3
MT 106	(20:31:33.60, 41:36:04)	B3V	4.4
MT 129	(20:31:41.60, 41:28:20)	B3V	4.6
MT 179	(20:31:59.80, 41:37:14)	B3V	4.9
MT 186	(20:32:03.00, 41:32:30)	B2Ve	4.2
MT 187	(20:32:03.70, 41:25:10)	B1V	5.3
MT 196	(20:32:05.60, 41:27:49)	B6V	4.4
MT 200	(20:32:06.80, 41:17:56)	B3V	6.5
MT 202	(20:32:07.90, 41:22:00)	B2V	4.7
MT 220	(20:32:14.60, 41:22:33)	B1V	5.3
MT 227	(20:32:16.50, 41:25:36)	O9V	4.1
MT 234	(20:32:19.70, 41:20:39)	B2V	4.5
MT 241	(20:32:22.10, 41:27:41)	B2V	4.0
MT 248	(20:32:25.50, 41:24:51)	B2V	4.6
MT 250	(20:32:26.10, 41:29:39)	B2III	3.8
MT 252	(20:32:26.50, 41:19:13)	B1.5III	4.9
MT 259	(20:32:27.80, 41:28:51)	B0Ib	3.7
MT 268	(20:32:31.40, 41:30:51)	B2.5V	4.9
MT 271	(20:32:32.30, 41:22:57)	B4V	5.0
MT 273	(20:32:32.50, 41:26:46)	B5:V	5.2
MT 275	(20:32:32.70, 41:27:04)	B2V	3.9
MT 295	(20:32:37.80, 41:26:15)	B2V	4.3
MT 311	(20:32:42.90, 41:20:16)	B2V	4.8
MT 317	(20:32:45.40, 41:25:37)	O8V	4.1
MT 339	(20:32:50.00, 41:23:44)	O8V	4.4

Table 3—Continued

Star Index	(R.A.,Dec.)	Spectral Type	Av
MT 365	(20:32:56.70, 41:23:40)	B1V	4.5
MT 372	(20:32:58.80, 41:04:29)	B0V	7.3
MT 376	(20:32:59.20, 41:24:25)	O8V	4.4
MT 390	(20:33:02.90, 41:17:43)	O8V	6.3
MT 395	(20:33:04.40, 41:17:08)	B1V	6.0
MT 400	(20:33:05.20, 41:17:51)	B1V	5.6
MT 409	(20:33:06.60, 41:21:13)	B0.5V	6.0
MT 429	(20:33:10.50, 41:22:22)	B0V	5.5
MT 444	(20:33:11.80, 41:24:05)	B5V	4.9
MT 448	(20:33:13.30, 41:13:28)	O6V	6.9
MT 453	(20:33:13.40, 41:26:39)	B5:V	3.9
MT 457	(20:33:14.20, 41:20:21)	O3If	4.9
MT 469	(20:33:15.50, 41:27:32)	B1III	4.9
MT 477	(20:33:17.40, 41:12:38)	B0:V	6.5
MT 488	(20:33:18.50, 41:15:35)	B1Ve-B3Ve	7.7
MT 507	(20:33:21.00, 41:17:40)	O9V	5.0
MT 509	(20:33:21.10, 41:35:52)	B0III-B0IV	6.1
MT 513	(20:33:22.50, 41:22:16)	B2V	4.9
MT 515	(20:33:23.20, 41:13:41)	B1V	6.8
MT 517	(20:33:23.40, 41:20:17)	B1V	5.2
MT 534	(20:33:26.80, 41:10:59)	O8.5V	6.0
MT 539	(20:33:27.20, 41:35:57)	B5:Ve	7.3
MT 554	(20:33:30.50, 41:20:17)	B4Ve	4.7
MT 568	(20:33:33.40, 41:08:36)	B3V	7.0
MT 576	(20:33:34.60, 41:21:37)	B7:V	4.6
MT 588	(20:33:37.00, 41:16:11)	B0V	5.8
MT 620	(20:33:42.40, 41:11:45)	B0V	6.2
MT 641	(20:33:47.60, 41:29:57)	B5V:	5.0
MT 642	(20:33:47.90, 41:20:41)	B1III	5.3
MT 645	(20:33:48.40, 41:13:14)	B2III	6.2

Table 3—Continued

Star Index	(R.A.,Dec.)	Spectral Type	Av
MT 646	(20:33:48.90, 41:19:40)	B1.5V	4.8
MT 745	(20:34:13.50, 41:35:02)	O7V	4.9
MT 759	(20:34:24.60, 41:26:24)	B1V	5.7
A11	(20:32:31.50, 41:14:08)	O7.5Ibf	7.7
A12	(20:33:38.20, 40:41:06)	B0Ia	8.2
A15	(20:31:36.80, 40:59:08)	O7Ibf	7.7
A18	(20:30:07.80, 41:23:49)	O8V	7.3
A23	(20:30:39.70, 41:08:48)	B0.7Ib	6.2
A25	(20:32:38.40, 40:40:44)	O8III	7.0
A26	(20:30:57.70, 41:09:56)	O9.5V	6.6
A29	(20:34:56.00, 40:38:17)	O9.7Iab	6.1
A32	(20:32:30.30, 40:34:32)	O9.5IV	5.9
A34	(20:31:36.90, 42:01:21)	B0.7Ib	4.8
A36	(20:34:58.70, 41:36:16)	B0Ib(n)sb2?	5.7
A37	(20:36:04.50, 40:56:12)	O5V	6.1
A38	(20:32:34.80, 40:56:17)	O8V	5.7
A41	(20:31:08.30, 42:02:42)	O9.7II	5.5
A42	(20:29:57.00, 41:09:52)	B0V	4.9
A45	(20:29:46.60, 41:05:08)	B0.5V(n)sb2?	4.3

Table 4. Spitzer and Akari Photometry

Star Index	J	H	Ks	IRAC1	IRAC2	IRAC3	IRAC4	9μm	MIPS24
MT 5	9.1(2)	8.57(2)	8.31(2)	8.2(3)	8.13(3)	8.14(5)	8.17(7)	···	···
MT 20	9.79(2)	9.19(2)	8.89(2)	8.7(2)	8.66(4)	8.62(7)	8.62(7)	···	···
MT 21	10.86(2)	10.5(2)	10.3(2)	10.2(3)	10.18(3)	10.18(5)	10.22(7)	···	9.33(5)
MT 42	10.86(2)	10.49(2)	10.24(2)	10.14(3)	10.08(6)	10.12(3)	10.15(6)	···	···
MT 83	8.08(2)	7.75(2)	7.63(2)	7.53(3)	7.49(3)	7.48(6)	7.48(5)	···	7.66(5)
MT 97	11.81(2)	11.42(2)	11.24(2)	11.15(3)	11.09(4)	11.06(5)	10.9(2)	···	···
MT 106	11.62(3)	11.19(2)	11(1)	10.88(3)	10.84(3)	10.85(5)	10.9(5)	···	···
MT 129	11.32(3)	10.89(2)	10.67(2)	10.54(4)	10.4(1)	10.5(4)	10.3(3)	···	···
MT 179	10.67(2)	10.27(2)	10.03(2)	9.96(3)	9.87(5)	9.86(13)	9.97(5)	···	8.21(5)
MT 186	11.21(2)	10.85(2)	10.63(2)	10.57(6)	10.5(4)	10.24(.3)	10.5(2)	···	···
MT 187	9.9(2)	9.49(2)	9.26(2)	9.32(6)	9.27(5)	9.21(19)	9.25(6)	···	8.64(5)
MT 196	11.49(2)	10.99(2)	10.74(2)	10.6(2)	10.6(2)	10.6(2)	10.6(2)	···	···
MT 200	9.62(2)	9.07(2)	8.79(2)	8.69(6)	8.58(5)	8.51(13)	8.56(8)	···	8.25(5)
MT 202	11.18(2)	10.79(2)	10.57(2)	10.47(3)	10.4(7)	10.43(3)	10.53(5)	···	···
MT 220	10.94(2)	10.48(2)	10.23(2)	10.12(4)	10.03(5)	10.08(4)	10.06(7)	···	···
MT 227	8.71(2)	8.39(3)	8.19(2)	8.12(4)	8.06(5)	8.08(5)	7.87(33)	···	···
MT 234	10.45(2)	10.1(2)	9.9(2)	9.83(5)	9.8(4)	9.81(3)	9.76(17)	···	8.71(5)
MT 241	10.75(2)	10.45(2)	10.27(2)	10.19(5)	10.17(4)	10.17(6)	10.1(2)	···	···
MT 248	10.47(2)	10.13(2)	9.92(2)	9.87(3)	9.81(3)	9.8(4)	9.73(4)	6.88	11.03(3)
MT 250	10.43(2)	10.15(2)	9.99(2)	9.95(4)	9.91(7)	9.8(22)	10.0(2)	···	···
MT 252	10.66(2)	10.23(2)	9.97(2)	9.81(4)	9.76(4)	9.78(4)	9.8(2)	···	···
MT 259	9.19(2)	8.9(2)	8.77(2)	8.75(5)	8.72(5)	8.73(7)	8.7(2)	···	8.92(5)

Table 4—Continued

Star Index	J	H	Ks	IRAC1	IRAC2	IRAC3	IRAC4	9μm	MIPS24
MT 268	10.94(2)	10.48(2)	10.24(2)	10.13(4)	10.08(6)	10.07(4)	10.4(5)	···	···
MT 271	11.12(2)	10.64(2)	10.41(2)	10.29(3)	10.24(4)	10.26(5)	10.23(5)	···	···
MT 273	12.05(2)	11.67(2)	11.46(2)	11.31(1)	11.3(1)	11.23(6)	11.1(2)	···	···
MT 275	11.05(2)	10.77(2)	10.61(2)	10.55(6)	10.49(9)	10.39(.3)	10.7(2)	···	···
MT 295	11.12(2)	10.75(2)	10.56(2)	10.5(3)	10.43(6)	10.5(3)	10.66(8)	···	···
MT 311	10.68(2)	10.21(2)	10(2)	9.93(8)	9.85(6)	9.87(6)	9.95(9)	···	···
MT 317	7.95(2)	7.62(2)	7.4(1)	7.42(4)	7.35(4)	7.37(3)	7.37(4)	···	7.7(2)
MT 339	8.58(2)	8.19(2)	7.98(2)	7.92(3)	7.87(4)	7.89(3)	7.87(3)	···	7.4(1)
MT 365	10.79(2)	10.36(2)	10.15(2)	10.08(3)	10.04(4)	10.0(2)	9.6(2)	···	6.38(5)
MT 372	10.51(2)	9.92(2)	9.6(2)	9.5(2)	9.36(3)	9.38(3)	9.4(4)	···	···
MT 376	8.89(3)	8.52(2)	8.31(2)	8.25(3)	8.19(4)	8.15(8)	8.21(4)	···	···
MT 390	8.72(3)	8.17(2)	7.87(2)	7.73(3)	7.67(3)	7.66(3)	7.66(4)	···	···
MT 395	10.27(2)	9.8(2)	9.55(1)	9.42(4)	9.35(5)	9.39(4)	9.6(1)	···	···
MT 400	10.61(2)	10.2(2)	9.94(1)	9.83(3)	9.76(4)	9.76(4)	9.5(2)	···	···
MT 409	10.39(2)	9.92(2)	9.67(1)	9.52(3)	9.45(7)	9.49(3)	9.6(1)	···	···
MT 429	9.54(2)	9.11(2)	8.9(1)	8.81(4)	8.78(3)	8.76(4)	8.71(8)	···	···
MT 444	10.42(2)	9.95(2)	9.7(1)	9.61(4)	9.52(9)	9.42(13)	9.56(7)	···	···
MT 448	8.98(3)	8.35(2)	8.01(2)	7.84(4)	7.77(3)	7.77(4)	7.83(5)	···	···
MT 453	11.49(2)	11.09(2)	10.9(1)	10.81(3)	10.75(4)	10.73(6)	10.7(4)	···	···
MT 457	7.25(2)	6.82(2)	6.61(2)	6.43(4)	6.34(5)	6.23(4)	6.14(4)	6.07	5.19(1)
MT 469	10.36(2)	9.93(2)	9.72(1)	9.62(4)	9.6(3)	9.54(17)	9.61(1)	···	···
MT 477	10.23(2)	9.68(1)	9.43(2)	9.3(4)	9.19(8)	9.23(6)	9.73(8)	···	7.05(5)

Table 4—Continued

Star Index	J	H	Ks	IRAC1	IRAC2	IRAC3	IRAC4	9μm	MIPS24
MT 488	9.41(2)	8.58(2)	7.98(1)	7.21(4)	6.9(3)	6.59(4)	6.19(6)	6.37	4.97(5)
MT 507	9.3(2)	8.9(2)	8.67(1)	8.58(6)	8.53(4)	8.55(3)	8.58(5)	···	···
MT 509	10.22(2)	9.68(2)	9.39(1)	9.23(3)	9.2(2)	9.17(4)	9.27(4)	···	···
MT 513	10.95(2)	10.55(2)	10.32(1)	10.23(3)	10.17(3)	10.2(2)	10.2(2)	···	···
MT 515	10.24(2)	9.68(2)	9.36(2)	9.23(5)	9.14(5)	9.19(8)	9.3(2)	···	···
MT 517	10.4(2)	10(2)	9.78(1)	9.7(4)	9.63(6)	9.6(18)	9.3(2)	···	···
MT 534	8.97(2)	8.43(2)	8.17(2)	8.05(3)	7.97(5)	7.9(1)	7.85(3)	···	7.5(2)
MT 539	9.58(2)	8.82(2)	8.18(1)	7.87(4)	7.49(3)	7.16(4)	6.68(3)	···	···
MT 554	11.03(2)	10.53(2)	10.3(1)	10.15(5)	10.12(4)	10.12(7)	10.16(6)	···	···
MT 568	10.28(2)	9.75(2)	9.42(2)	9.28(5)	9.22(4)	9.17(8)	9.1(16)	···	···
MT 576	11.59(2)	11.18(2)	10.93(1)	10.8(8)	10.74(3)	10.7(5)	10.7(4)	···	···
MT 588	8.68(2)	8.17(2)	7.93(1)	7.8(6)	7.72(4)	7.7(3)	7.64(6)	···	···
MT 620	9.89(2)	9.38(2)	9.1(2)	9(3)	8.94(3)	8.93(1)	9.1(2)	···	5.47(5)
MT 641	10.09(2)	9.63(2)	9.33(2)	9.23(5)	9.18(3)	9.2(14)	9.3(2)	···	···
MT 642	7.99(2)	7.49(2)	7.21(2)	7.08(3)	7.01(3)	6.95(4)	6.92(5)	6.88	8.31(5)
MT 645	10.58(2)	10.07(2)	9.78(2)	9.66(4)	9.6(3)	9.53(13)	9.62(6)	···	···
MT 646	10.03(2)	9.62(2)	9.37(2)	9.29(3)	9.21(5)	9.2(1)	9.17(7)	···	···
MT 745	8.55(2)	8.15(2)	7.92(2)	7.85(3)	7.8(3)	7.82(4)	7.83(3)	···	···
MT 759	10.87(2)	10.38(2)	10.11(2)	9.99(3)	9.91(4)	9.94(4)	9.9(5)	···	6.31(5)
A11	7.82(2)	7.09(2)	6.66(2)	6.3(6)	6.16(6)	6.16(3)	6.04(5)	6.3	5.58(1)
A12	6.9(2)	6.17(2)	5.75(2)	5.45(3)	5.34(4)	5.19(5)	5.24(7)	5.32	4.89(5)
A15	7.91(2)	7.21(2)	6.81(2)	6.55(3)	6.42(3)	6.29(3)	6.24(3)	6.44	6.14(1)

Table 4—Continued

Star Index	J	H	Ks	IRAC1	IRAC2	IRAC3	IRAC4	9μm	MIPS24
A18	9.4(2)	8.74(2)	8.37(2)	8.17(4)	8.08(3)	8.07(3)	8.07(7)	···	···
A23	6.93(2)	6.33(2)	5.98(2)	5.72(6)	5.62(4)	5.48(4)	5.45(5)	5.58	5.19(5)
A25	8.35(3)	7.71(2)	7.38(2)	7.21(3)	7.13(3)	7.09(6)	7.09(3)	7.63	···
A26	9.09(2)	8.51(2)	8.2(1)	8.02(4)	7.95(3)	7.95(4)	7.82(4)	···	···
A29	7.44(2)	6.86(2)	6.55(2)	6.25(4)	6.16(2)	6.13(6)	6.05(3)	···	···
A32	7.89(2)	7.37(2)	7.07(2)	6.82(4)	6.79(7)	6.8(3)	6.79(4)	6.88	7(1)
A34	7.36(2)	6.96(2)	6.66(2)	6.55(3)	6.49(4)	6.4(5)	6.33(4)	···	···
A36	7.19(2)	6.66(2)	6.36(2)	6.32(3)	6.19(4)	6.04(6)	5.94(4)	5.8	···
A37	8.57(3)	7.97(2)	7.69(2)	7.53(8)	7.43(3)	7.4(3)	7.38(5)	6.99	···
A38	9.38(2)	8.86(2)	8.56(2)	8.48(6)	8.4(5)	8.4(7)	8.37(6)	···	···
A41	7.83(2)	7.29(2)	7.02(2)	6.75(4)	6.7(2)	6.69(3)	6.67(3)	6.37	···
A42	9.12(2)	8.7(2)	8.45(2)	8.33(4)	8.29(4)	8.3(3)	8.28(7)	···	···
A45	9.03(2)	8.64(2)	8.46(2)	8.42(3)	8.38(5)	8.37(8)	8.4(2)	···	···

Table 5. Table of SED fitting results

Star Index	Spectral Type	δAv	χ^2_R SM	DC	SW	T_d	γ	Group
MT 5	O6V	5.65	1.2	···	1.5	···	0.99	A
MT 20	B0V	6.60	1.5	···	···	···	···	A
MT 21	B2II	4.40	5.1	0.7	5.3	150	0.90	B
MT 42	B2V	4.22	0.5	···	···	···	···	A
MT 83	B1I	3.40	42.3	17.7	···	1950	···	D
MT 97	B2V	4.30	1.4	···	···	···	···	A
MT 106	B3V	4.40	1.5	···	···	···	···	A
MT 129	B3V	4.78	0.4	···	···	···	···	A
MT 179	B3V	4.55	65.6	3.4	53.5	50	0.90	C
MT 186	B2Ve	4.38	0.6	···	···	···	···	A
MT 187	B1V	4.95	9.3	6.2	9.0	150	0.90	D
MT 196	B6V	5.10	0.8	···	···	···	···	A
MT 200	B3V	5.80	1.4	···	2.0	···	0.90	A
MT 202	B2V	4.52	0.4	···	···	···	···	A
MT 220	B1V	5.30	0.5	···	···	···	···	A
MT 227	O9V	4.28	0.8	···	1.0	···	0.99	A
MT 234	B2V	4.15	18.6	2.0	15.5	150	0.90	B(?)
MT 241	B2V	3.82	0.7	···	···	···	···	A
MT 248	B2V	4.25	13.1	17.5	···	1950	···	D
MT 250	B2III	3.45	0.4	···	···	···	···	A
MT 252	B1.5III	5.08	0.2	···	···	···	···	A
MT 259	B0Ib	3.35	7.2	5.7	···	1950	···	D
MT 268	B2.5V	5.08	0.9	···	···	···	···	A
MT 271	B4V	4.65	2.3	···	···	···	···	A(?)
MT 273	B5:V	4.50	1.0	···	···	···	···	A
MT 275	B2V	3.72	0.2	···	···	···	···	A
MT 295	B2V	4.12	1.2	···	···	···	···	A
MT 311	B2V	4.80	1.3	···	···	···	···	A
MT 317	O8V	3.92	2.7	···	3.2	···	0.99	A(?)
MT 339	O8V	4.58	2.3	···	2.8	···	0.99	A(?)

Table 5—Continued

Star Index	Spectral Type	δAv	χ^2_R SM	χ^2_R DC	χ^2_R SW	T_d	γ	Group
MT 365	B1V	4.68	>1000	3.4	>1000	150	0.90	B(?)
MT 372	B0V	6.60	0.9	···	···	···	···	A
MT 376	O8V	4.58	1.1	···	1.4	···	0.99	A
MT 390	O8V	6.12	1.2	···	1.4	···	0.99	A
MT 395	B1V	5.65	1.2	···	···	···	···	A
MT 400	B1V	4.90	1.6	···	···	···	···	A
MT 409	B0.5V	5.30	0.3	···	···	···	···	A
MT 429	B0V	4.80	1.7	···	···	···	···	A
MT 444	B5V	4.72	1.4	···	···	···	···	A
MT 448	O6V	6.72	1.8	···	2.2	···	0.99	A
MT 453	B5:V	4.08	1.5	···	···	···	···	A
MT 457	O3If	4.55	0.8	···	1.0	···	0.99	A
MT 469	B1III	4.55	1.4	···	···	···	···	A
MT 477	B0:V	5.80	777.1	15.2	277.0	150	0.90	D
MT 488	B1Ve-B3Ve	8.40	>1000	171.0	>1000	350	0.90	D
MT 507	O9V	4.82	1.8	···	2.2	···	0.99	A
MT 509	B0III-B0IV	5.92	2.0	···	···	···	···	A
MT 513	B2V	4.55	0.9	···	···	···	···	A
MT 515	B1V	6.10	0.7	···	···	···	···	A
MT 517	B1V	4.85	0.5	···	···	···	···	A
MT 534	O8.5V	5.82	2.7	···	2.8	···	0.99	A(?)
MT 539	B5:Ve	8.71	108.0	7.0	37.3	350	0.90	D
MT 554	B4Ve	4.88	2.1	···	···	···	···	A(?)
MT 568	B3V	6.30	4.5	5.3	···	50	···	D
MT 576	B7:V	4.42	0.9	···	···	···	···	A
MT 588	B0V	5.80	2.4	···	···	···	···	A(?)
MT 620	B0V	5.85	>1000	3.1	>1000	50	0.90	B(?)
MT 641	B5V:	4.82	3.1	···	···	···	···	A(?)
MT 642	B1III	4.60	262.9	141.0	···	1950	···	D
MT 645	B2III	5.50	2.3	···	···	···	···	A(?)

Table 5—Continued

Star Index	Spectral Type	δAv	χ^2_R SM	DC	SW	T_d	γ	Group
MT 646	B1.5V	4.98	1.0	···	···	···	···	A
MT 745	O7V	4.72	1.8	···	2.2	···	0.99	A
MT 759	B1V	5.52	>1000	1.2	>1000	150	0.90	B
A11	O7.5Ibf	7.52	3.7	3.9	4.5	550	0.99	D
A12	B0Ia	7.85	55.0	1.1	2.7	550	1.06	B
A15	O7Ibf	6.64	214.1	60.0	226.0	800	0.99	D
A18	O8V	7.30	1.2	···	1.5	···	0.99	A
A23	B0.7Ib	6.55	57.3	0.9	5.5	550	1.10	B
A25	O8III	6.65	1.1	···	1.3	···	0.99	A
A26	O9.5V	6.42	1.9	···	2.2	···	0.99	A
A29	O9.7Iab	6.45	3.4	2.2	4.1	200	0.99	B(?)
A32	O9.5IV	5.90	7.2	3.9	6.0	550	0.99	B(?)
A34	B0.7Ib	4.80	6.8	1.1	3.2	350	0.90	B
A36	B0Ib(n)sb2?	5.35	14.1	5.0	11.4	250	0.90	C
A37	O5V	6.28	0.3	···	0.4	···	0.99	A
A38	O8V	5.88	1.8	···	2.1	···	0.99	A
A41	O9.7II	5.50	3.1	2.7	3.4	400	0.99	B(?)
A42	B0V	5.08	0.7	···	···	···	···	A
A45	B0.5V(n)sb2?	4.30	1.7	···	···	···	···	A

Note. — SM: Stellar Model DC: Stellar Model with Dust Component SW: Stellar Model with Stellar Wind Component T_d: Fitted Dust Component temperature γ: γ used in the Stellar Wind component fit